Molecular Biology of the Cell
Vol. 21, 3093–3105, September 15, 2010

Functional Relationship between Protein Disulfide Isomerase Family Members during the Oxidative Folding of Human Secretory Proteins

Lori A. Rutkevich, Myrna F. Cohen-Doyle, Ulf Brockmeier,* and David B. Williams

Department of Biochemistry, University of Toronto, Toronto, Canada M5S 1A8

Submitted April 26, 2010; Accepted July 8, 2010
Monitoring Editor: Benjamin S. Glick

To examine the relationship between protein disulfide isomerase family members within the mammalian endoplasmic reticulum, PDI, ERp57, ERp72, and P5 were depleted with high efficiency in human hepatoma cells, either singly or in combination. The impact was assessed on the oxidative folding of several well-characterized secretory proteins. We show that PDI plays a predominant role in oxidative folding because its depletion delayed disulfide formation in all secretory proteins tested. However, the phenotype was surprisingly modest suggesting that other family members are able to compensate for PDI depletion, albeit with reduced efficacy. ERp57 also exhibited broad specificity, overlapping with that of PDI, but with preference for glycosylated substrates. Depletion of both PDI and ERp57 revealed that some substrates require both enzymes for optimal folding and, furthermore, led to generalized protein misfolding, impaired export from the ER, and degradation. In contrast, depletion of ERp72 or P5, either alone or in combination with PDI or ERp57 had minimal impact, revealing a narrow substrate specificity for ERp72 and no detectable role for P5 in oxidative protein folding.

INTRODUCTION

Proteins entering the secretory pathway are initially targeted to the endoplasmic reticulum (ER) where protein folding and posttranslational modifications take place in a specialized environment. Critical among these modifications is the formation, isomerization, and reduction of disulfide bonds catalyzed by thiol oxidoreductases of the protein disulfide isomerase (PDI) family. Assignment of as many as 20 proteins to the mammalian PDI family is based on the presence of at least one thioredoxin-like domain, with catalytic activity determined by the presence of a pair of cysteine residues within a CXXC motif that is able to alternate between disulfide and dithiol forms (Appenzeller-Herzog and Ellgaard, 2008; Hatahet *et al*., 2009). To act as an oxidase and form disulfide bonds, the active site must itself be oxidized, whereas reduction and isomerization events are carried out when the active site is reduced. Although relatively few substrates have been examined in detail, it appears that disulfide isomerization is a slow process that may be rate-limiting in the folding of certain proteins. In vitro studies on the oxidative folding of bovine pancreatic trypsin inhibitor revealed that partially disulfide-bonded intermediates become kinetically trapped during folding and that isomerization of disulfides was the main process responsible for the >1000-fold enhancement in folding rate observed in the presence of PDI (Weissman and Kim, 1993). Furthermore, in vivo studies have shown that both the HIV-1 envelope glycoprotein (Land *et al*., 2003) and low-density lipoprotein receptor (Jansens *et al*., 2002) form a number of incorrect disulfide bonds early in folding and that posttranslational isomerization events are then required for reshuffling and native folding.

PDI was the first ER thiol oxidoreductase to be characterized (Goldberger *et al*., 1964), and its oxidase and isomerase activities have been validated in vitro (Lyles and Gilbert, 1991), in yeast (Laboissiere *et al*., 1995; Kulp *et al*., 2006), and in mammalian systems (Bulleid and Freedman, 1988). The structure of yeast PDI reveals a U-shaped orientation of its four thioredoxin-like domains, termed *a*, *b*, *b*′, and *a*′, where *a* and *a*′ denote the catalytically active domains containing the CXXC motif and *b* and *b*′ are noncatalytic domains (Kemmink *et al*., 1997; Tian *et al*., 2006). The *b*′ domain appears to be the main site for substrate binding and for the reported chaperone functions of PDI (Klappa *et al*., 1998; Horibe *et al*., 2004). There is a hydrophobic surface within the interior of the U structure that is provided by the *b*′ domain as well as the other domains that appears well suited for interaction with nonnative folding intermediates (Tian *et al*., 2006). Indeed, direct interactions between a hydrophobic pocket in the *b*′ domain of PDI spanning residues 240–320 and the amphipathic peptides mastoparan

This article was published online ahead of print in *MBoC in Press* (http://www.molbiolcell.org/cgi/doi/10.1091/mbc.E10–04–0356) on July 21, 2010.

* Present address: Institut für Physiologie, Universität Duisburg-Essen, Hufelandstrasse 55, 45122 Essen, Germany.

Address correspondence to: David B. Williams (david.williams@utoronto.ca).

Abbreviations used: α_1AT, α_1-antitrypsin; αFP, α-fetoprotein; α_2HS, α_2HS glycoprotein; Alb, albumin; Cnx, calnexin; Crt, calreticulin; DTT, dithiothreitol; ERAD, ER-associated degradation; NEM, N-ethylmaleimide; PDI, protein disulfide isomerase; TF, transferrin; UPR, unfolded protein response.

and somatostatin, as well as with unfolded RNase A, have been documented recently in NMR titration studies (Denisov *et al.*, 2009). On substrate oxidation, the catalytic sites of PDI are reduced and must be reoxidized for subsequent rounds of catalysis. This is accomplished by the FAD-binding oxidase Ero1 that donates oxidizing equivalents to PDI in both yeast (Sevier and Kaiser, 2002) and mammals (Mezghrani *et al.*, 2001; Wang *et al.*, 2009). PDI has also been implicated in maintaining redox homeostasis as a feedback regulator of Ero1 (Appenzeller-Herzog *et al.*, 2008) and by retaining Ero1 in the ER (Otsu *et al.*, 2006). Although PDI carries out all the functions of a thiol oxidoreductase in the ER, many other enzymes in this family can catalyze these reactions in vitro (Alanen *et al.*, 2006). Consequently, there has been great interest in determining the extent to which PDI family members exhibit functional overlap versus unique properties such as restricted substrate specificities.

This issue has been addressed in *S. cerevisiae* that possesses five PDI family members of which only PDI is essential. In most instances, the ability of individual family members to restore viability to a PDI-deleted strain, when overexpressed, required low level expression of one of the other homologues. Furthermore, only PDI was capable of supporting native folding of the carboxypeptidase Y substrate (Norgaard *et al.*, 2001). These findings indicate little functional interchangeability within yeast PDI homologues and underscore the predominant role of PDI in catalyzing oxidative folding of substrates.

Similar studies in mammalian cells have been hampered by the plethora of homologues and by the difficulties in maintaining cell viability when PDI levels are constitutively depleted (Park *et al.*, 2006). However, transient PDI knockdown experiments have implicated this enzyme in facilitating cholera toxin retrotranslocation from ER to cytosol whereas the related family members ERp57 and ERp72 either had no effect or an opposing effect, respectively (Forster *et al.*, 2006). Furthermore, PDI, but not ERp57, has been shown to affect the production of infectious rotavirus particles (Maruri-Avidal *et al.*, 2008) and the folding of human MHC class I heavy chains (Kang *et al.*, 2009). Additional studies have focused on those members that most closely resemble PDI. Of these, the best characterized is ERp57 which shares a high degree of similarity with PDI, but its substrate-binding *b′* domain has diverged such that it interacts with the ER lectin-chaperones calnexin (Cnx) and calreticulin (Crt) (Oliver *et al.*, 1999; Kozlov *et al.*, 2006). These chaperones are thought to present glycoprotein substrates to ERp57, and indeed, ERp57 has a well-established specificity for Asn-linked glycoproteins that is abrogated when its interactions with Cnx and Crt are disrupted (Zapun *et al.*, 1998; Jessop *et al.*, 2009a). Nevertheless, there are several reports of ERp57 acting directly on a few select substrates independently of a requirement for Cnx or Crt (Peaper *et al.*, 2005; Schelhaas *et al.*, 2007; Zhang *et al.*, 2009). Studies in which ERp57 has been depleted through RNA interference or gene knockout have established that ERp57 is required for the efficient oxidative folding of mouse MHC class I heavy chains (Zhang *et al.*, 2006), influenza hemagglutinin (Solda *et al.*, 2006), clusterin, and β1 integrin (Jessop *et al.*, 2007).

Another family member, ERp72, contains three catalytic and two noncatalytic domains (Mazzarella *et al.*, 1990) and, although it shares high sequence similarity with ERp57, it is not able to bind to Cnx or Crt (Kozlov *et al.*, 2009). Limited information is available concerning a functional relationship between ERp72 and ERp57. ERp72 was unable to substitute functionally for ERp57 in the oxidative folding of MHC class I molecules (Zhang *et al.*, 2006) but it did replace ERp57 in mixed disulfide complexes with several glycoprotein substrates when ERp57 was either eliminated or its recruitment to substrates by Cnx/Crt impaired by treatment with castanospermine (Solda *et al.*, 2006; Jessop *et al.*, 2009b). Additionally, ERp72 has been implicated in the folding of thyroglobulin (Menon *et al.*, 2007) and apolipoprotein B (Linnik and Herscovitz, 1998), but no consensus has been reached as to how ERp72 recognizes substrates. Finally, P5 is a poorly understood member of the PDI family with one noncatalytic and two catalytic domains (Rupp *et al.*, 1994). Although found in a large multi-enzyme complex that also includes PDI, ERp72, and BiP (Meunier *et al.*, 2002), only recently has it been implicated in a direct interaction with BiP, possibly mediating its substrate selection (Jessop *et al.*, 2009b).

Despite these findings, the question of why so many PDI family members exist in the ER remains enigmatic. The hypothesis of differences in substrate specificity has been impressively investigated using substrate-trapping mutants of PDI family members in which the second cysteine in the CXXC active site motif is mutated to alanine. This inactivates an escape pathway in which the second cysteine thiolate resolves mixed disulfide intermediates between the first cysteine and substrate (Walker and Gilbert, 1997). These studies revealed distinct substrate profiles for each PDI family member but with considerable overlap (Jessop *et al.*, 2009a; Jessop *et al.*, 2009b). Most notable was a strong preference for glycoprotein substrates by ERp57, a surprisingly wide range of substrates for P5 and an equally surprising dearth of identifiable substrates for PDI. As welcome as this information is, the approach has a number of limitations: substrate identification is difficult, trap mutants are overexpressed and must compete with endogenous enzymes for substrate, the functional role of individual family members cannot be assessed, and, because trap mutants do not permit the CXXC motif to become oxidized, substrates undergoing PDI member-catalyzed oxidative folding are not detected.

To address some of these issues, we report the first systematic knockdown of multiple PDI family members in mammalian cells and its functional consequences on the oxidative folding and intracellular trafficking of a number of endogenously expressed substrates, including albumin, α-fetoprotein, transferrin, α_2-HS-glycoprotein, and α_1-antitrypsin. By high efficiency depletion of PDI, ERp57, ERp72, and P5, either alone or in various combinations, we assess their relative importance in oxidative folding as well as their functional overlap when evaluated with a common group of substrates.

MATERIALS AND METHODS

Cell Lines and Antibodies

HepG2 cells were maintained in high glucose DMEM containing 10% fetal bovine serum (FBS) and antibiotics. This was supplemented with either 1 μg/ml puromycin (Bioshop, Toronto, ON, Canada) or 200 μg/ml hygromycin B (Invitrogen, Carlsbad, CA) for HepG2 cells stably expressing ERp57 shRNAmir or mutant PDI, respectively. Antibodies used in this study were as follows: anti-PDI and -ERp72 (AssayDesigns, Plymouth Meeting, PA), anti-P5 (Affinity Bioreagents, Cambridge, United Kingdom), anti-BiP (BD Biosciences, Franklin Lakes, NJ), anti-CHOP (Thermo, Rockford, IL), anti-actin (Chemicon, Temecula, CA), anti-albumin, -transferrin and -α_1-antitrypsin (Sigma, St. Louis, MO) and anti-α-fetoprotein and -α_2-HS-glycoprotein (Abcam, Cambridge, MA). Rabbit antisera directed against calnexin, calreticulin, and ERp57 have been described previously (Danilczyk and Williams, 2001; Zhang *et al.*, 2006; Ireland *et al.*, 2008). The 12CA5 anti-HA mAb was provided by Dr. Tania Watts (University of Toronto).

Human PDI cDNA Isolation and Mutagenesis

mRNA was isolated from HepG2 cells and then cDNA was produced using the RevertAid H Minus kit (Fermentas, Burlington, ON, Canada). Using this as template, cDNA encoding PDI with an HA tag inserted after position D499,

five residues upstream of the C-terminal KDEL sequence, was amplified using primer pair PDI-forward: 5′-ATATATAAGCTTGCGGCCGC*GCCAC*-CatgCTGCGCCGC-GCTCTGCTGTGCC-3′ and PDI-reverse-1: 5′-**AGCGT-AATCTGGAACATCGTATGG-GTA**ATCGTCTTCCTCCATGTCTGGCTC-3′. These primers encode 5′ NotI and HindIII sites (underlined), a Kozak sequence (italics), start codon (lower case) and the HA-tag (bold). This PCR product was used as template in a second PCR with primer pair PDI-forward and PDI-reverse-2: 5′-ATATATGGATCCttaCAGTTCATCTTTCACAG-CTTTCTGATC**AGCGT-AATCTGGAACATCGTATGGGTA**-3′ to amplify the complete PDI cDNA and encode the remainder of PDI following the HA-tag (bold) including the stop codon (lower case) and a BamHI site (underlined). The product was digested with HindIII and BamHI and ligated into pBluescript+ (Stratagene, La Jolla, CA), producing pBS-PDI^{WT}.

To generate the double mutant PDI-C56A, C400A (PDI^{CXXA}-HA), a modified QuikChange mutagenesis protocol was performed (Zheng *et al.*, 2004) using plasmid pBS-PDI^{WT} as template and the following primer pairs: C56A-forward: 5′-GTGTGGCCACgcC*AAaGCTtT*GGCCCCTGAGTATGCCAAAG-3′ and C56A-reverse: 5′-CAGGGGCC*AaAGCtTT*GgcGTGGCCACACCAAGGGGCATAG-3′; and C400A-forward: 5′-GTGTGGTCACgcCAAACAGTTGGCTCCCATTTG-3′ and C400A-reverse: 5′-CACTGTTT-GgcGTGACCACACCATGGGGCATAG-3′ (mutagenic nucleotides in lower case, mutated codons underlined, silent restriction site in italics). The constructs encoding PDI^{WT}-HA and PDI^{CXXA}-HA were subcloned into plasmid pQCXIH (Clontech, Mountain View, CA) using NotI/BamHI sites. Recombinant Moloney virus packaged with the respective pQCXIH plasmids was used to infect HepG2 cells (Ireland *et al.*, 2008), with stable transformants selected in 200 μg/ml hygromycin B.

RNA Interference

Stealth Select siRNAs (40 nM final; Invitrogen), either specific for PDI, ERp57, ERp72, or P5, or a negative nontargeting control, were mixed with 6 μL of Oligofectamine (Invitrogen) in a final volume of 500 μL of Opti-MEM medium in 6-well plates. To each well, 2.5×10^5 HepG2 cells in 1.5 ml of DMEM were added and, after 4 h at 37°C, the medium was supplemented with 1 ml DMEM and FBS to a final concentration of 10%. After knockdown for 3 d, the cells were trypsinized, pooled, and resuspended for a second transfection with fresh complexes using the same targeting siRNA. After an additional 3 d, cells were prepared for analysis. For transfections with two different siRNAs, the above protocol was carried out but treatment with each siRNA was staggered by one day, extending the total time to 7 d.

For constitutive knockdown of ERp57, recombinant Moloney virus packaged with pSM2c-ERp57shRNAmir (OpenBiosystems, Huntsville, AL) was used to infect HepG2 cells as described above. Transformants were subjected to a second infection with virus as well as clonal selection to maximize knockdown efficiency. Double and triple knockdowns were carried out in this cell line using siRNAs as described above.

Unfolded Protein Response Induction and RT-PCR

Positive controls for unfolded protein response (UPR) induction were carried out by treating HepG2 cells with either 0.5 or 5 μg/ml tunicamycin (Sigma) dissolved in DMSO or an equivalent volume of DMSO only (control) overnight at 37°C. Cells were split for immunoblot analysis and for RNA isolation. Total RNA was subjected to one-step reverse transcription PCR (Qiagen, Chatsworth, CA) using human Xbp-1 amplification primers: 5′-GGAGTTAA-GACAGCGCTTGG-3′ and 5′-GAGATGTTCTGGAGGGGTGA-3′.

Metabolic Radiolabeling and Immunoisolation

After RNAi, HepG2 cells (1×10^6) were starved for 30 min with Met-free RPMI 1640 and radiolabeled for 3 min in 1 ml of medium containing 0.1 mCi of [^{35}S]Met (>1000 Ci/mmol; Perkin Elmer, Boston, MA). The cells were chased for various times in RPMI 1640 supplemented with 1 mM Met and then incubated on ice for 3 min in 2 ml of PBS supplemented with 20 mM N-ethylmaleimide (NEM; Sigma). Cells were then lysed at 4°C in 1 ml RIPA buffer (50 mM Tris pH 7.4, 150 mM NaCl, 1 mM EDTA, 1% NP-40, 0.25% Na-deoxycholate (DOC), 0.1% SDS, and protease inhibitors) containing 20 mM NEM and subjected to serial immunoisolations with 30 μg anti-albumin, anti-transferrin, anti–α-fetoprotein, anti–α-2-HS-glycoprotein, and anti–α-1-antitrypsin antibodies. In each case, following 2 h at 4°C, immune complexes were recovered by incubation for 1 h with 30 μL of protein-A agarose beads (GE Healthcare, Little Chalront, Buckinghamshire, United Kingdom). Agarose-bound immune complexes were washed four times with 50 mM Tris pH 7.4, 150 mM NaCl, 1 mM EDTA, 0.1% NP-40, 0.025% DOC, 0.01% SDS and split for elution in SDS-PAGE sample buffer either lacking or containing 40 mM DTT. Samples were analyzed by SDS-PAGE (10% gels), detected using a Storm phosphorimager (Molecular Dynamics; GE Healthcare), and quantified with ImageQuant software (GE Healthcare).

For sequential immunoisolation of mixed disulfide complexes between PDI^{CXXA}-HA and substrates, HepG2 cells expressing mutant PDI or the viral vector were pulsed for 15 min with 50 μCi/plate of [^{35}S]Met, incubated with PBS containing 20 mM NEM, and lysed as outlined above. Immunoisolation was carried out using anti-HA antibody and protein-A agarose with immune complexes eluted and disrupted by incubation at 40°C for 1 h in 0.2% SDS in PBS (pH 6.8). The eluates were adjusted to 2% NP-40, 5 mg/ml gelatin, and 50 μM HA peptide (Genscript, Piscataway, NJ) in PBS (pH 6.8) before a second round of immunoisolation with anti-substrate antibody. Immune complexes were analyzed by reducing SDS-PAGE (10% gel) and visualized by fluorography.

RESULTS

Effective Knockdown of PDI Family Members without Observable UPR Induction

Because attempts have failed to obtain mammalian cell lines that constitutively express very low levels of PDI (Park *et al.*, 2006), a transient RNAi knockdown approach was used to assess the functions of PDI family members in human hepatoma cells. For high efficiency knockdown, it was necessary to carry out the knockdown over a period of 6 d with two transfections of the targeting siRNA. Cell growth was equivalent in both control and knockdown conditions after the first transfection, but following the second application of siRNA a slowing of growth rate was observed in cells treated with targeting siRNA compared with cells treated with control siRNA (~75% of control rate for PDI knockdown and ~85% for knockdown of other PDI family members). However, no accompanying loss of cell viability or impairment of protein translation was observed (data not shown).

Using the two-step transfection method, >95% knockdown efficiency was attained for PDI, ERp57, ERp72, and P5 using either of two independent siRNAs (Figure 1A). HepG2 cells constitutively expressing shRNA targeting ERp57 (ERp57^{sh}) also exhibited knockdown of ERp57 comparable to that observed with siRNA. These cells facilitated experiments in which both ERp57 and a second or third PDI family member were depleted in combination. Knockdown efficiency also exceeded 95% in the various combination knockdowns (Figure 1A). No off-target knockdown was observed for other PDI family members, and in no case was compensatory upregulation of remaining family members observed.

We anticipated that depletion of PDI family members might induce the UPR. Surprisingly, there was no increase in the expression of BiP, PDI or CHOP, representing middle and late stages of the UPR, in any of the single or multiple knockdowns (Figure 1A) (Wu and Kaufman, 2006). Additionally, there was no alteration in the levels of Cnx or Crt. To monitor the IRE-1 pathway directly, we tested for Xbp-1 splicing (Yoshida, 2007), and the spliced product was not observed in any of the knockdown conditions compared with cells treated with tunicamycin as a positive control (Figure 1B). Similarly, there was no evidence of PERK pathway activation as measured by phosphorylation of eIF2α (data not shown).

We further tested whether PDI-depleted cells might be more susceptible to externally imposed ER stress. HepG2 cells were subjected to knockdown for an extended period of ten days including an additional siRNA transfection on day 6 to maintain cellular siRNA concentration. As shown in Figure 1C, greater than 95% knockdown of PDI was maintained during this period, yet remarkably there was no evidence of UPR induction as assessed either by Xbp-1 splicing or by increased BiP expression (Figure 1C, compare lanes 1 and 4). These cells were subsequently tested for their sensitivity to ER stress induced by tunicamycin. Control cells exhibited Xbp-1 splicing and a 1.4-fold increase in BiP level only at 5 μg/ml tunicamycin, but in 10-d PDI-depleted cells Xbp-1 splicing and increased BiP expression (1.5-fold) were apparent at a 10-fold lower concentration of tunicamycin. Furthermore, at 5 μg/ml tunicamycin, the increase in BiP level (1.9-fold) and extent of Xbp-1 splicing in PDI-depleted cells exceeded those observed in control cells (Fig-

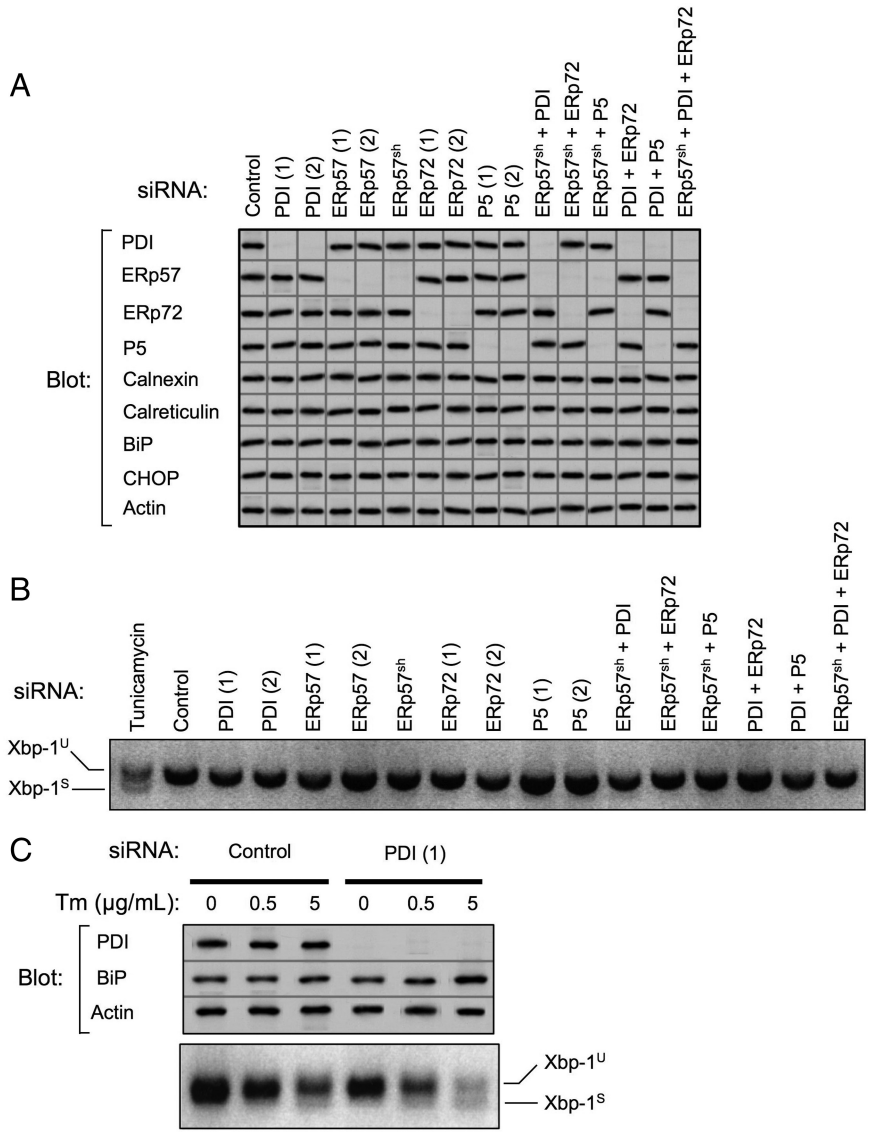

Figure 1. Efficacy of PDI family member knockdown and assessment of UPR. (A) PDI family members were depleted from HepG2 cells by RNAi over a period of 6 d. Indicated single or multiple knockdowns were carried out transiently using two independent targeting siRNAs, designated (1) and (2), or in some instances using cells constitutively expressing shRNAmir targeting ERp57 ($ERp57^{sh}$). Equivalent amounts of cell lysates were immunoblotted for PDI family members, ER chaperones, CHOP, and actin. Images shown are a composite from various experiments, all of which included actin as a loading control. Exposures were adjusted to an equivalent density of the actin control. Data are representative of a minimum of five replicate knockdowns. (B) After the indicated knockdowns or overnight treatment with 5 μg/ml tunicamycin, total RNA was isolated from HepG2 cells and analyzed for Xbp-1 splicing by reverse-transcription PCR. $Xbp\text{-}1^{U}$, unspliced Xbp-1 product; $Xbp\text{-}1^{S}$, spliced Xbp-1 product. (C) HepG2 cells were subjected to PDI knockdown for 10 d. On day 9, cells were treated overnight with the indicated concentrations of tunicamycin (Tm). The following day, cell lysates were immunoblotted to detect PDI, BiP, and actin. Lanes shown were assembled from a single gel. Total RNA was also isolated and analyzed for Xbp-1 splicing.

ure 1C). These findings indicate that HepG2 cells depleted of PDI, although not exhibiting an overt UPR themselves, are more sensitive to ER stress imposed through tunicamycin treatment. Because the degree of Xbp-1 splicing and BiP upregulation in control HepG2 cells was remarkably modest after tunicamycin treatment (Figure 1C), it may be that these professional secretory cells have higher basal levels of folding and ER-associated degradation (ERAD) machineries, and so they do not respond as readily as other cell types to stress conditions. Indeed, it has been reported that nearly 75% of endogenous apolipoprotein B-100 in HepG2 cells is constitutively degraded cotranslationally (Adeli *et al*., 1997), suggesting that misfolded substrates may be disposed of without the need for an additional UPR.

The preceding data indicate that the 6-d period chosen for PDI family member depletion is suitable to assess the functions of PDI family members without confounding factors such as compensatory upregulation of other family members or induction of the UPR.

Identification of PDI Substrates

Human HepG2 cells were selected for these experiments because they express many well characterized secretory proteins that possess disulfide bonds. Albumin (Alb), α-fetoprotein (αFP), and transferrin (TF) are attractive study subjects since they are monomeric, contain multiple disulfides, and have molecular weights sufficiently low for oxidative folding to be monitored by nonreducing SDS-PAGE. Furthermore, αFP and TF are glycosylated whereas Alb is not, which permits an assessment of glycoprotein preference by PDI family members during catalysis of oxidative folding. To first confirm that these secretory proteins are indeed substrates of PDI, HepG2 cells were prepared that constitutively express an HA-tagged substrate-trapping mutant of PDI (PDI^{CXXA}-HA) (Figure 2A). Mutation of the second Cys in both PDI active sites stabilizes mixed-disulfide reaction intermediates with substrates on which it is acting as a reductase or isomerase (Walker and Gilbert, 1997). Although our focus is on oxidative folding, it is likely that in the case of PDI it selects substrates largely through hydrophobic interactions regardless of the reaction catalyzed (Tian *et al*., 2006). Radiolabeled cells expressing PDI^{CXXA}-HA were subjected to a first round of immunoisolation with anti-HA mAb followed by disruption of immune complexes and a second round of immunoisolation with Ab directed against

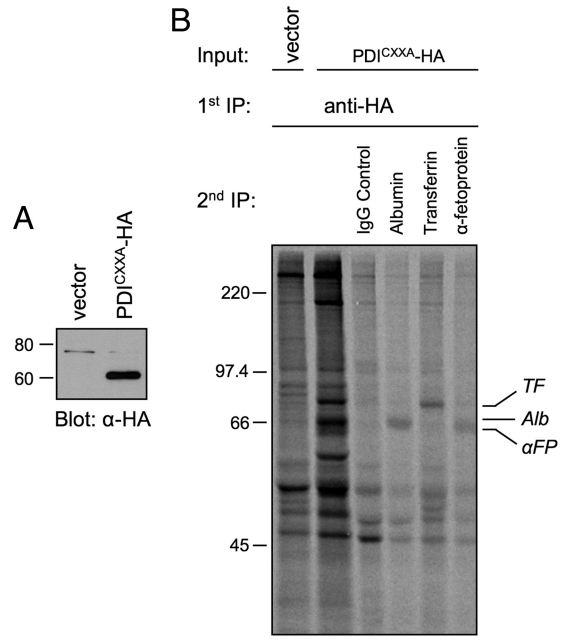

Figure 2. Identification of PDI substrates. (A) Lysates of HepG2 cells stably expressing either the pQCXIH expression vector (vector) or HA-tagged PDI carrying C56A and C400A mutations (PDI^{CXXA}-HA) were immunoblotted with anti-HA antibody. (B) HepG2 cells expressing either vector or PDI^{CXXA}-HA were radiolabeled with [^{35}S]Met for 15 min, and treated with 20 mM NEM in PBS. Cell lysates were immunoisolated with anti-HA antibody, immune complexes were disrupted and then immunoisolated a second time with the indicated antibodies. Proteins were separated by reducing SDS-PAGE and visualized by fluorography. Alb, albumin; αFP, α-fetoprotein; TF, transferrin.

various secretory proteins. As shown in Figure 2B, Alb, αFP, and TF could all be recovered as complexes with the PDI trap mutant, confirming them as PDI substrates. Other bands observed in complex with the PDI trap mutant were not identified but presumably correspond to additional PDI substrates (Figure 2B, lane 2). In addition to Alb, αFP, and TF, α_2-HS-glycoprotein (α_2HS) was selected for study based on high disulfide content and available reagents. As a negative control to detect any pleiotropic effects of PDI family member knockdown, α_1-antitrypsin (α_1AT) was selected because it is a glycoprotein that lacks disulfide bonds.

Individual Knockdown of PDI Family Members

To determine the contributions of PDI, ERp57, ERp72, and P5 to the oxidative folding of secretory proteins, pulse-chase experiments were carried out under control and knockdown conditions. Free thiols were alkylated with membrane-permeable NEM before cell lysis to prevent air oxidation and disulfide isomerization. As shown for PDI knockdown in Figure 3A, nonreducing SDS-PAGE was used to monitor the progression of substrate proteins from the fully reduced (R) form of slow mobility to partially oxidized (PO) and fully oxidized forms (O) of higher mobilities. For αFP and α_2HS, the fully oxidized form was further converted to one or two slower-mobility species (G, G_1), reflecting processing of their oligosaccharide chains to larger complex structures in the Golgi. A reduction in signal was also apparent at late chase times due to secretion, and fully oxidized species could be recovered from the culture medium (Figure 3B). These were included when calculating percentages of proteins oxidized or secreted (Figure 3, B and C). In addition, the region near the top of the gel as well as the stacking gel were monitored for disulfide-linked aggregates, because previous PDI and ERp57 depletion studies involving overexpressed exogenous substrates had reported significant quantities of such aggregates (Solda *et al*., 2006; Lee *et al*., 2010). However, we did not observe disulfide-linked aggregates upon PDI family member depletion, either individually or in combination, for any of our endogenous substrates (shown only for Alb in Figures 3–6).

During the oxidative folding of Alb and αFP, formation of disulfide bonds was very rapid and a substantial shift in gel mobility was seen even in the 3 min pulse period (Figure 3A, control; compare lane P -/+ DTT). Only one distinct partially oxidized species was observed under control conditions that slowly progressed to fully oxidized forms (species O and G) over the course of 30–60 min. On depletion of PDI, the impact on oxidative folding was remarkably modest for both proteins. The initial rapid formation of the partially oxidized species during the 3-min pulse period was unchanged, but progression to the fully oxidized species during the subsequent 10 min of chase was delayed (Figure 3A, PDI lanes and Figure 3C, dashed lines). No other partially oxidized forms were observed. By 20–30 min of chase, the proportion of fully oxidized Alb and αFP (O + G species) in PDI-depleted cells became similar to that in control cells, although it was noted that in the PDI-depleted cells the conversion of the αFP O species to the Golgi-processed G species was delayed. Because nonnative protein conformers are normally subject to quality control and retained in the ER, we also monitored secretion rates and, in the case of glycoproteins, ER to Golgi transport rates as an indirect measure of folding efficiency. This method has been used previously to detect incorrectly disulfide-bonded conformers in proteins that exhibit an otherwise normal extent of oxidation (Chakravarthi and Bulleid, 2004; Solda *et al*., 2006). Both Alb and αFP appeared in the culture medium at similar rates in the absence or presence of PDI (Figure 3B). ER to Golgi transport of αFP was measured by the rate at which its oligosaccharides were processed from an endo H-sensitive ER form to a complex endo H–resistant form in the *medial*-Golgi (Figure 3D, quantified in Figure 3E). In the absence of PDI, ER to Golgi transport of αFP was notably delayed at the 30 min chase time, consistent with the delay noted above in the conversion of the αFP O species to the G species at 30 min in Figure 3A. Because control experiments revealed no delay in the ER to Golgi transport of nondisulfide-bonded α_1-antitrypsin (α_1AT), the delay observed for αFP was specific to this protein. Given that αFP exhibited a similar degree of disulfide formation at the 30 min chase point in the absence or presence of PDI (Figure 3C), these data are consistent with the presence of nonnative folding intermediates that may require a disulfide isomerization event, delayed in the absence of PDI, to be released from the ER quality control machinery.

The oxidative folding of TF occurred at a slower pace than Alb or αFP, and the fully oxidized form was not detectable until 10 min of chase under control conditions (Figure 3, A and C). Multiple partially oxidized folding intermediates were visible as a smear between the fully reduced and fully oxidized forms. On depletion of PDI, the formation of the various partially oxidized species appeared unaffected but the rate of their subsequent conversion to the fully oxidized species was delayed. However, by 60 min of chase, TF was maximally oxidized in both control and PDI-depleted cells. PDI-depletion also resulted in slower ER to Golgi transport of TF, most apparent by 60 min of chase (Figure 3, D and E), although no difference in its rate of secretion was detected

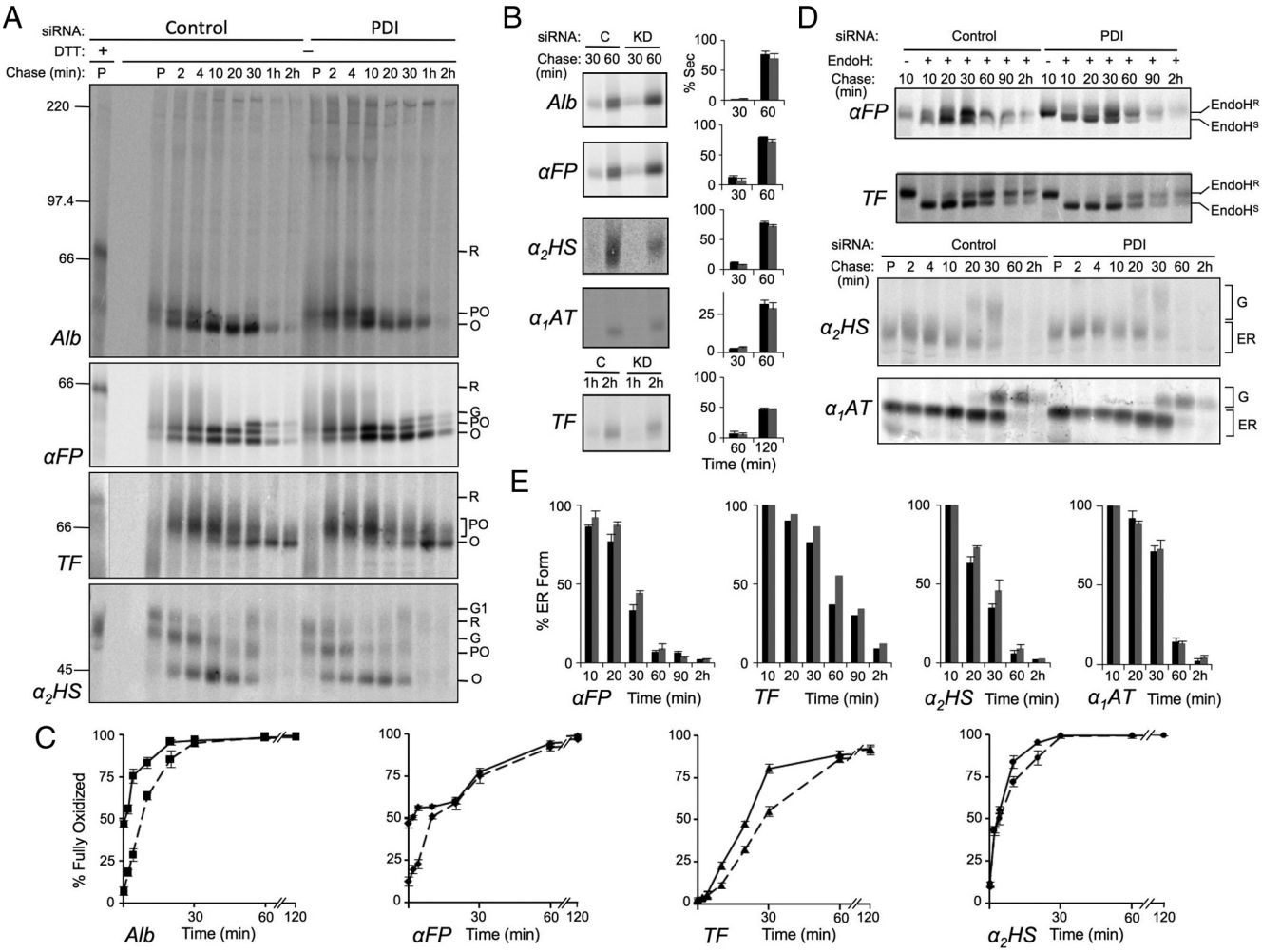

Figure 3. Effect of PDI knockdown on oxidative folding of secretory proteins. HepG2 cells were depleted of PDI or treated with control siRNA for 6 d, radiolabeled with [^{35}S]Met for 3 min, then chased with unlabeled Met for the indicated times. The medium was removed, and then cells were treated on ice with 20 mM NEM in PBS and lysed in RIPA buffer containing 20 mM NEM. Both cell lysates and media were immunoisolated with antisera directed against the indicated proteins. (A) Kinetics of disulfide formation. Immune complexes from cell lysates were subjected to SDS-PAGE under reducing (first lane) or nonreducing conditions and proteins were visualized and quantified by phosphorimaging. Shown are representative gels of three independent experiments for substrates albumin (Alb), α-fetoprotein (αFP), transferrin (TF), and α_2-HS-glycoprotein (α_2HS). Reduced (R), partially oxidized (PO), oxidized (O), and Golgi (G, G1) forms of each protein are indicated. (B) Secretion kinetics. Immune complexes recovered from media samples at the indicated chase times were analyzed by SDS-PAGE and visualized and quantified by phosphorimaging. Histograms indicate the amount of protein observed in the medium as a percentage of the combined intra- and extracellular signal at each chase time. Black and gray bars represent control (C) and knockdown (KD) conditions, respectively. (C) Quantification of gels shown in panels A and B was carried out by expressing the amount of fully oxidized protein in lysate and media samples as a percentage of the total combined amount of reduced, partially oxidized, and oxidized forms at a given time point. Solid lines represent control conditions; dashed lines represent knockdown conditions. (D) ER to Golgi transport kinetics. The indicated proteins were immunoisolated and either digested or not with endo H as indicated and analyzed by reducing SDS-PAGE. Endo H^S and Endo H^R represent endo H–sensitive and -resistant species, respectively. G and ER represent Golgi-processed and ER forms which could be resolved without endo H digestion. (E) Quantification of the gels in panel D. Histograms represent the amount of protein remaining in the ER as a percentage of the total protein recovered from cells and medium at each time point. Black bars, control; gray bars, knockdown. Error bars represent the average of three independent experiments ± one SD, except in the case of TF which was examined in a single experiment.

(Figure 3B). The final secretory protein tested, α_2HS, yielded clearly distinguishable fully reduced, partially oxidized, and fully oxidized forms, but only a slight delay in oxidative folding was observed at the 10- and 20-min chase times in PDI-depleted cells (Figure 3, A and C). By 30 min of chase, α_2HS was fully oxidized (species O, G, G_1) in both control and PDI-depleted cells. A modest delay in ER to Golgi transport was also observed in PDI-depleted cells at 20 and 30 min of chase (Figure 3, D and E). It is noteworthy that slower ER to Golgi transport was manifested for both TF and α_2HS at time points when they were maximally oxidized, again suggestive of nonnative disulfides in the absence of PDI.

Overall, PDI appears to be a versatile and prominent oxidoreductase in that its depletion affected all substrates tested and other PDI family members could not fully complement its loss. However, the phenotypes observed were more modest than expected given the essential role of PDI in yeast, raising the question of whether other PDI family members are able to substitute to some degree for the functions of PDI.

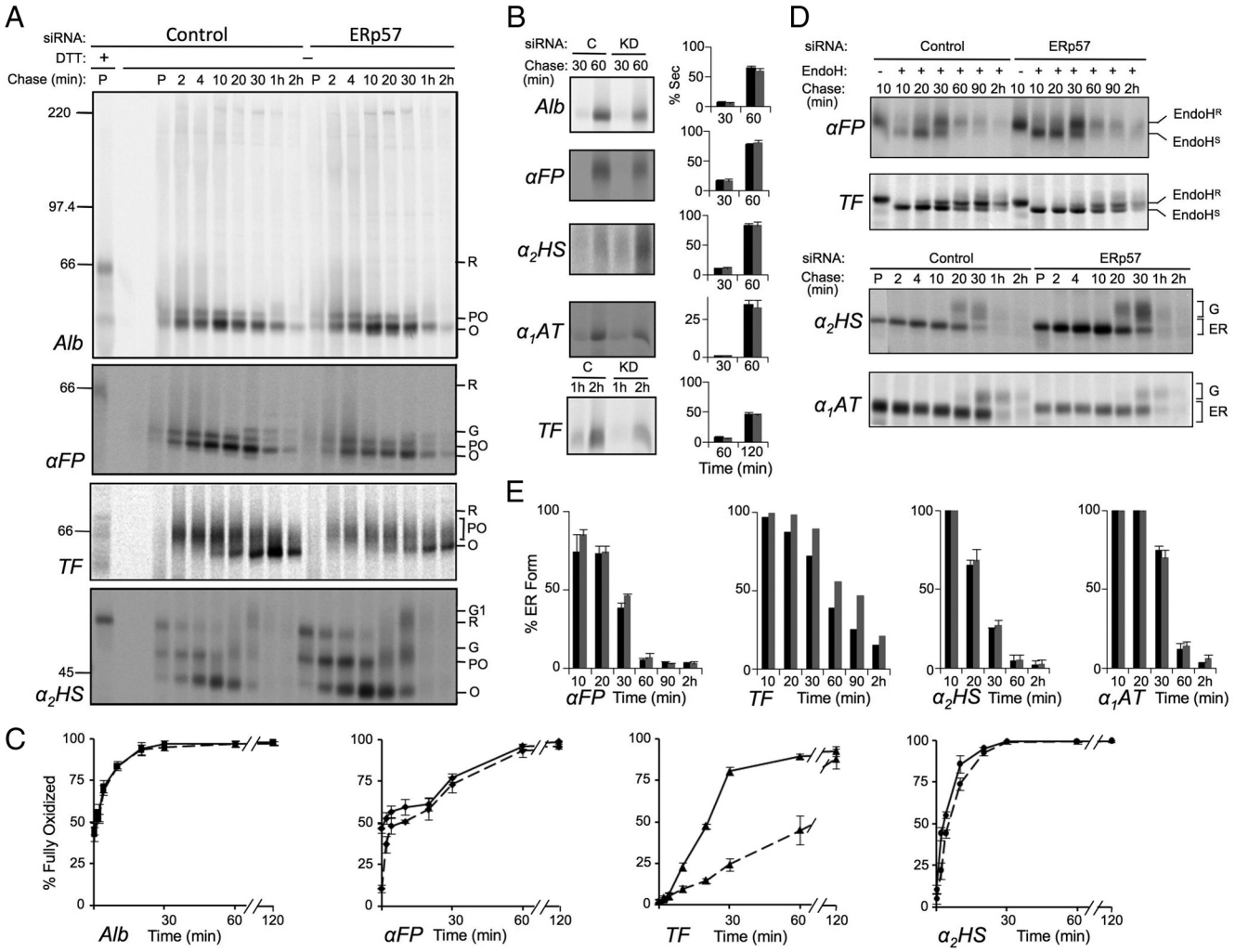

Figure 4. ERp57 depletion delays oxidative folding of glycosylated substrates. HepG2 cells were depleted of ERp57 or treated with control siRNA and pulse-chase experiments were conducted and analyzed as described in Figure 3. (A) Kinetics of disulfide formation. (B) Secretion kinetics. Black and gray bars represent control and knockdown conditions, respectively. (C) Quantification of oxidative folding. Solid lines, control conditions; dashed lines, knockdown conditions. (D) ER to Golgi transport kinetics. (E) Quantification of the gels in panel D. Error bars represent the average of three independent experiments ± one SD, except in the case of TF which was examined in a single experiment.

We next knocked down ERp57 and monitored the same substrates for changes in oxidative folding and intracellular transport. For Alb there was no observed difference in oxidative folding in cells with or without ERp57 and no changes in secretion efficiency (Figure 4, A–C). In contrast, αFP and α_2HS, exhibited modest delays in oxidative folding similar to those observed upon depletion of PDI. However, unlike PDI depletion, there was little impact on rates of ER to Golgi transport, suggesting that native disulfides were being formed (Figure 4, D and E). For TF, ERp57 depletion resulted in a marked delay in oxidative folding that was considerably more pronounced than that observed with PDI depletion (Figure 4, A–C). This occurred through 60 min of chase, at which time only 45% of transferrin had reached a fully oxidized state in the absence of ERp57 compared with 85% fully oxidized transferrin in PDI-depleted cells (compare Figures 3C and 4C). By 2h, almost all of TF in the cells and medium was fully oxidized (Figure 4, A–C, TF panel). Although secretion of TF was not significantly delayed upon ERp57 depletion, ER to Golgi transport was substantially impaired (Figure 4, D and E). This was observed throughout 30–90 min of chase, reflecting the slower formation of disulfide bonds. These data indicate that TF is a substrate highly specific to ERp57 and that other family members, such as PDI, are acting on this substrate with reduced efficacy. Even the modest phenotypes observed upon ERp57 depletion for αFP and α_2HS suggest that PDI, despite being able to act on these substrates, is not able to fully complement the loss of ERp57 for these client proteins. The lack of impact of ERp57 depletion on the folding of Alb stands in contrast to the other substrates. Alb is the only protein in this set that is not glycosylated and hence is less likely to be targeted via Cnx or Crt to ERp57 (Jessop *et al*., 2009a). This is in agreement with previous work suggesting that the action of ERp57 is largely specific for glycoproteins (Oliver *et al*., 1999; Solda *et al*., 2006; Jessop *et al*., 2009a).

Individual knockdowns of ERp72 and P5 were also carried out. However, there was no change in the oxidative folding of any of the substrates tested and no changes were observed in their rates of ER to Golgi transport or secretion (data summarized in Table 1). Because the preceding data indicated that the secretory proteins under study are substrates for PDI and/or ERp57, it is possible that any contribution of ERp72 or P5 to the oxidative folding of these

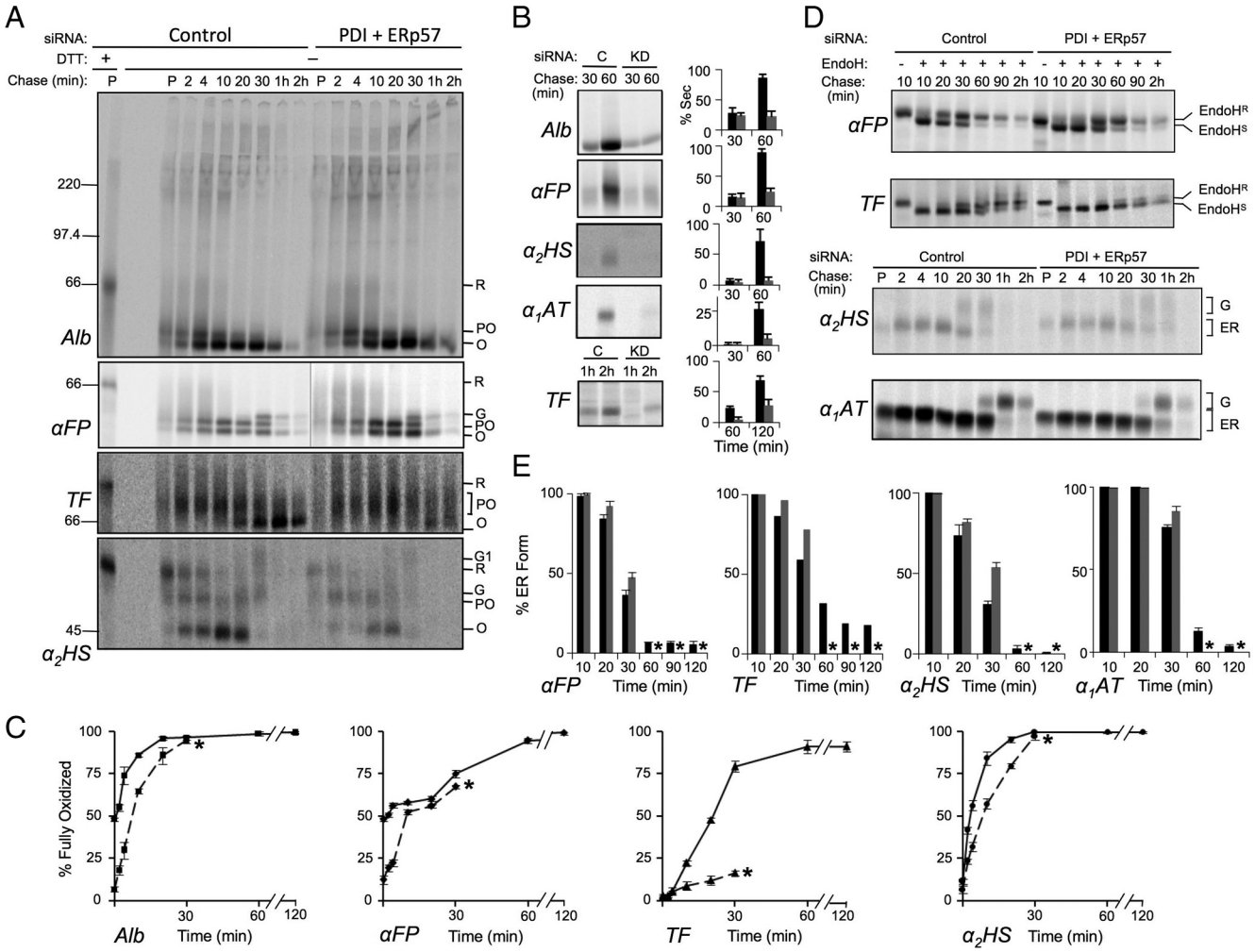

Figure 5. Combined knockdown of PDI and ERp57 substantially impairs protein folding. HepG2 cells constitutively depleting ERp57 by shRNAmir were subjected to knockdown of PDI by siRNA for 6 d. HepG2 cells transfected with control siRNA were prepared in parallel. Pulse-chase experiments were conducted and analyzed as described in Figure 3. (A) Kinetics of disulfide formation. (B) Secretion kinetics. Amount secreted was quantified as a percentage of the total signal recovered at the 10 min chase time point. Black and gray bars represent control and knockdown conditions, respectively. (C) Quantification of oxidative folding. Solid lines, control conditions; dashed lines, knockdown conditions. (D) ER to Golgi transport kinetics. (E) Quantification of the gels in panel D. Error bars represent the average of three independent experiments ± one SD, except in the case of TF which was examined in a single experiment. Asterisks indicate quantifications were not included beyond 30 min of chase due to substrate degradation.

proteins was simply masked by the action of PDI or ERp57. Alternatively, ERp72 and P5 may not act on these substrates but are specific for other client proteins. To distinguish between these possibilities as well as to characterize the degree of functional overlap between PDI and ERp57, PDI family members were depleted in combination.

Combined Knockdown of PDI Family Members

Initially, PDI and ERp57 were knocked down with high efficiency (Figure 1A). As shown in Figure 5, A and B and quantified in Figure 6A, we observed a marked decrease in the total radioactive signal recovered from cell lysates and medium in double-knockdown cells beyond 30 min of chase, consistent with degradation of all substrate proteins (explored further below). Because this degradation complicated the determination of the percentage of fully oxidized or ER-localized forms of the substrates at later time points, quantifications were carried out up to the 30-min time point but not beyond (indicated by the asterisks in Figure 5, C and E). Additionally, the amount of each substrate secreted was quantified as a percentage of the total radioactive signal recovered at the 10-min chase time rather than as a percentage of the total signal recovered at each chase time. Figure 5, A and C shows that the oxidative folding of Alb was delayed to the same extent as when PDI alone was depleted, supporting our finding that ERp57 is not acting on this nonglycosylated substrate (Figure 4). For the glycoprotein substrates, a range of impairments in oxidative folding was observed. For αFP, there was little change relative to PDI or ERp57 depletion alone. For α_2HS, there was a greater delay in oxidative folding compared with that observed with either of the single knockdowns and, in the case of TF, oxidative folding was profoundly impaired. By 30 min of chase, only 15% of TF was fully oxidized compared with 25 and 50% when either PDI or ERp57 were depleted, respectively (compare Figures 3C, 4C, and 5C). Even after 2 h of chase, only small amounts of fully oxidized TF could be observed (Figure 5A). Furthermore, both secretion and ER to Golgi

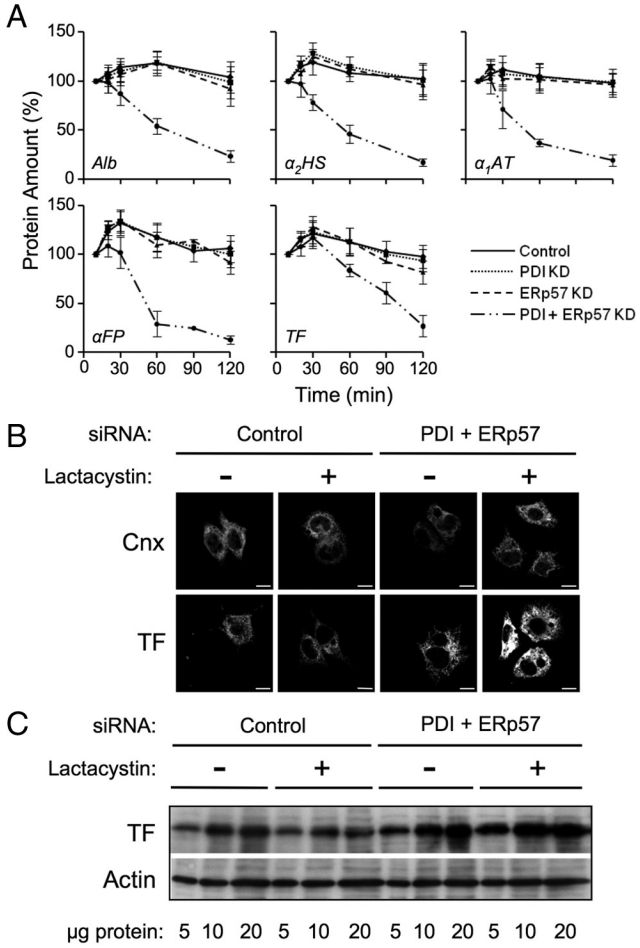

Figure 6. Misfolded transferrin is degraded by the proteasome in PDI/ERp57-depleted cells. (A) Pulse-chase data from Figures 3–5 was analyzed for changes in the total amount of radiolabeled Alb, αFP, TF, α_2HS, and α_1AT recovered from the combined intracellular and medium fractions. Total protein, as measured by densitometry, was defined as 100% at the 10 min chase time. Error bars represent the average of three independent experiments ± one SD. (B, C) HepG2 cells were treated with control siRNA or depleted of PDI and ERp57 for 6 d and then incubated in the absence or presence of 5 μg/ml lactacystin for 5 h. Cells were either plated on Cell-Tak-treated coverslips (BD Biosciences), fixed in paraformaldehyde, and permeabilized for confocal microscopy (B) or lysed in RIPA buffer for Western blot analysis (C). Immunoblot or immunofluorescence was carried out using the indicated antibodies (Scale bar = 10 μm).

transport were strongly impaired for all proteins tested (Figure 5, B, D, and E). On comparison to the α_1AT control, it was further observed that even a secretory protein lacking disulfide bonds was delayed both in its trafficking from ER to Golgi and its secretion. This suggests that combined depletion of ERp57 and PDI leads to a generalized impairment of ER function. The observed degradation of substrate proteins (Figure 6A) was investigated further in the case of TF by treating control and PDI/ERp57-depleted cells with the proteasome inhibitor lactacystin and examining both the subcellular distribution of TF by immunofluorescence microscopy and its steady state levels by immunoblotting. As shown in Figure 6B, ER morphology as assessed by Cnx staining was not grossly altered upon combined PDI and ERp57 depletion either alone or after treatment with lactacystin. TF exhibited a reticular ER staining pattern in both control and PDI/ERp57-depleted cells. However, staining was more intense in the depleted cells consistent with ER accumulation and the intensity increased substantially upon inhibition of proteasomal degradation. This was confirmed by immunoblotting wherein cellular levels of TF increased 2.2-fold upon combined PDI and ERp57 depletion relative to control cells and threefold following lactacystin treatment (Figure 6C). These data are consistent with a substantial degree of protein misfolding accompanying the combined loss of PDI and ERp57 and the subsequent disposal of misfolded proteins by ERAD. Such efficient disposal of misfolded proteins by HepG2 cells may explain the absence of an observable UPR upon depletion of PDI and ERp57 (Figure 1, A and B).

Collectively, the stronger phenotypes observed in the double versus single knockdown studies support the view that both PDI and ERp57 are involved in the oxidative folding of the glycoprotein substrates and that neither can fully replace the functions of the other. Furthermore, in the context of the mild phenotypes observed with the other combinatorial knockdowns (see below and Table 1), these experiments underscore the prominent role that these thiol oxidoreductases play among the four PDI family members examined.

We next tested whether depletion of ERp72 or P5 in combination with PDI would yield enhanced defects in folding. The combination of PDI + P5 showed no differences for any of the four substrates tested compared with data obtained for PDI knockdown alone (Table 1). For the PDI + ERp72 knockdown combination, oxidative folding profiles were comparable to PDI-depleted cells for the three glycoprotein substrates. In contrast, there was a more pronounced delay in the oxidative folding of Alb compared with PDI-depletion alone suggesting that both enzymes can act on this substrate (compare Figure 3, A and C and Figure 7). Unlike the PDI + ERp57 combination, these cells did not display a generalized delay in ER to Golgi trafficking or in secretion rate; indeed, the rate of Alb secretion was the same in both control and PDI + ERp72 knockdown cells (data not shown). Therefore, ERp72 likely recognizes a more limited set of substrates compared with PDI or ERp57. Its effect on Alb was likely masked in the individual ERp72 knockdown by the presence of PDI.

To assess whether an effect of ERp72 or P5 knockdown could be assigned in the absence of ERp57, combination knockdowns of ERp57 + ERp72 as well as ERp57 + P5 were carried out. There was no change observed in the oxidative folding of the four substrates beyond what had been noted for ERp57 knockdown alone (Table 1). Because the presence of PDI in these cells may have yet been influencing our ability to observe the impact of these family members on glycoprotein folding, a triple knockdown was carried out, depleting cells of PDI, ERp57, and ERp72. Remarkably, the cells grew and remained viable and behaved as previously observed for the PDI + ERp57 double knockdown. Alb oxidation was delayed in a manner similar to what had been observed in the PDI + ERp72 combination, but there was no additional change in the oxidative folding of the glycoproteins due to ERp72 depletion (Table 1). This again suggests that ERp72 does not act on these substrates but is specific for others such as Alb. The inability to detect any effect of P5 depletion may indicate specificity for a narrow range of substrates, none of which were included in this study, or that it may be involved in other processes such as substrate reduction.

Table 1. Summary of oxidative folding defects accompanying single and combined PDI family member knockdown

Substrate	MW (kDa)	Glycosylation sites (N-linked)	PDI	ERp57	ERp72	P5
Albumin	66	0	++	−	−	−
α-Fetoprotein	66	1	++	++	−	−
Transferrin	77	2	++	+++	−	−
α_2-HS glycoprotein	44	2	+	+	−	−
α_1-Antitrypsin	52	3	−	−	−	−

Substrate	ERp57/PDI	ERp72/PDI	PDI/ERp57/ERp72	ERp57/ERp72	ERp57/P5	PDI/P5
Albumin	++	+++	+++	−	−	++
α-Fetoprotein	++	++	++	++	++	++
Transferrin	++++	++	++++	+++	+++	++
α_2-HS glycoprotein	++	+	++	+	+	+
α_1-Antitrypsin	+	−	+	−	−	−

The degree of delay in formation of the fully oxidized protein substrate and/or its ER to Golgi trafficking rate in response to the indicated individual or combined PDI family member knockdowns is scored from −, signifying no effect, to ++++, signifying a profound delay.

DISCUSSION

Our current understanding of the relationships among mammalian PDI family members comes mainly from the use of substrate trap mutants to examine the spectrum of client proteins acted on by individual family members (Jessop *et al*., 2007; Jessop *et al*., 2009b). However, this approach does not detect substrates undergoing oxidative folding nor does it permit an assessment of the functional impact of each family member. Some functional studies on select substrates have been undertaken by depletion of individual family members but comparative assessment of the impact of depleting different PDI members on oxidative folding has been very limited (Solda *et al*., 2006; Kang *et al*., 2009; Zhang *et al*., 2009). The present study represents the first systematic comparison of the functions of mammalian PDI, ERp57, ERp72, and P5 in the oxidative folding of multiple endogenous substrates.

One of our more surprising findings is that depletion of PDI in HepG2 cells had a relatively modest impact on the oxidative folding capacity of the ER. For all substrates tested, oxidative folding was delayed rather than arrested, with the half-time for acquisition of the fully oxidized state being extended from less than twofold for the α_2HS and TF substrates to approximately eightfold for Alb and αFP. A trivial explanation is that low levels of PDI remaining after knockdown can still catalyze substantial disulfide formation. However, this possibility is unlikely given that estimates of PDI activity required to maintain yeast viability range from 10 to 20% (Hatahet *et al*., 2009), far higher than the trace levels detectable in our experiments. Rather, the modest phenotypes we observe are consistent with a substantial degree of redundancy among mammalian PDI family members, although they were not able to fully complement PDI deficiency. Interestingly, less redundancy is observed in yeast where PDI is absolutely required for efficient oxidative folding of carboxypeptidase Y; none of the remaining family members could support carboxypeptidase Y folding and maturation to even 50% of the efficiency observed with PDI (Norgaard *et al*., 2001). We also noted that PDI depletion resulted in a delay in ER to Golgi transport of αFP, α_2HS, and TF. This occurred after the acquisition of an apparent fully oxidized state, suggesting the presence of nonnative disulfides and hence a role for PDI in catalyzing disulfide isomerization. This is consistent with the finding that the isomerase activity of yeast PDI is required for efficient carboxypeptidase folding in vivo (Xiao *et al*., 2004). Despite the relative subtlety of the folding defects observed upon loss of PDI, it is noteworthy that PDI silencing affected the oxidation of all substrates examined, irrespective of their glycosylation status. This observation is in agreement with the generally held view that PDI is the predominant ER thiol oxidoreductase (Hatahet *et al*., 2009), directly binding to most folding proteins via hydrophobic interactions mediated largely through its *b′* domain (Pirneskoski *et al*., 2004; Tian *et al*., 2006).

The modest delay in oxidative folding upon PDI depletion is also surprising given that oxidizing equivalents within the ER are thought to pass from Ero1 through PDI to substrate protein (Sevier and Kaiser, 2008). Although controversial (Mezghrani *et al*., 2001), there is mounting evidence that other

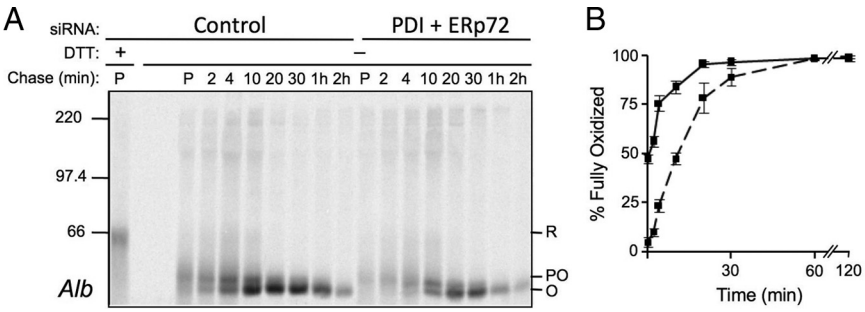

Figure 7. Effect of combined PDI and ERp72 knockdown on oxidative folding of albumin. HepG2 cells were depleted of PDI and ERp72 by siRNA or treated with control siRNA for 6 d and then subjected to pulse-chase radiolabeling and immunoisolation of Alb as described for Figure 3. (A) Representative gel of Alb oxidation from three independent knockdown experiments. (B) Quantification of gel shown in panel A. Solid lines, control conditions; dashed lines, knockdown conditions. Error bars represent the average of three independent experiments ± one SD.

PDI family members such as ERp57, ERp46, and ERp18 form mixed disulfides with Ero1 and hence may accept oxidizing equivalents in a similar manner (Jessop *et al*., 2009b). Alternatively, because more than half of ER-localized glutathione has been shown to be in the form of mixed disulfides with protein (Bass *et al*., 2004), this may serve as an alternative source of oxidative equivalents in the absence of PDI.

Our studies suggest that ERp57 is a leading candidate among PDI family members for activities that partially complement PDI deficiency. ERp57 had the broadest substrate specificity of the remaining PDI family members examined in this study, contributing to the efficient oxidative folding of αFP, α_2HS, and TF but not of Alb. Furthermore, when ERp57 was depleted in combination with PDI, a greater impairment in oxidative folding rates was observed for both TF and α_2HS compared with either single knockdown alone and slower export of all substrates from the ER was apparent along with evidence of misfolding and disposal by ERAD. Such extensive effects on protein folding and trafficking were not observed when either ERp72 or P5 was depleted in combination with PDI, although a greater delay in the oxidation of Alb was noted with combined PDI and ERp72 knockdown. These findings indicate overlapping substrate specificities for PDI and ERp57 as well as illustrating that both enzymes are required for the efficient folding of certain substrates, most notably TF. The generalized impairment of protein export from the ER and disposal by ERAD upon depletion of PDI and ERp57, but not with either enzyme individually, suggests that both enzymes are required for the folding of many other substrates as well. Our findings indicate that, of the four PDI family members examined, PDI and ERp57 contribute most substantially to oxidative protein folding within the ER. It will be of considerable interest in the future to test the generality of this observation with an expanded set of glycosylated and nonglycosylated substrates as well as other PDI family members.

Why might an individual substrate require the activities of both PDI and ERp57 during oxidative folding? One possibility is that individual substrate thiols exhibit substantial variation in redox potential that require different PDI family members for thiol-disulfide exchange reactions. However, both PDI and ERp57 possess similar reduction potentials that are substantially more oxidizing than those of substrate thiols (reviewed in (Hatahet *et al*., 2009), rendering such a requirement unlikely. Another possibility is that one enzyme acts primarily to catalyze disulfide formation whereas the other is more involved in isomerization reactions. However, current evidence supports the ability of PDI and ERp57 to catalyze both types of reactions in vivo (Xiao *et al*., 2004 and see below) and further work would be required to determine whether this varies from one substrate to another. Perhaps a more likely possibility is that PDI and ERp57 recognize distinct substrate conformers during the folding process. This may occur either through direct interaction with hydrophobic patches on the substrate in the case of PDI or indirectly through association with different chaperones. As discussed below, ERp57 is thought to be recruited to folding glycoproteins primarily through its association with Cnx and Crt which recognize nonnative folding intermediates by virtue of a lectin site specific for monoglucosylated oligosaccharides as well as through a hydrophobic polypeptide binding site (Williams, 2006). PDI has also been detected in a large complex that contains BiP and Grp94, both of which may influence PDI-substrate interactions (Meunier *et al*., 2002). Such distinct modes of substrate recognition may dictate the utilization of PDI or ERp57 at different stages of the substrate folding pathway.

Previous studies using substrate-trapping mutants of ERp57 (Jessop *et al*., 2007) or that interfered with the formation of ERp57-Cnx/Crt (Jessop *et al*., 2009a) or Cnx/Crt-glycoprotein complexes (Oliver *et al*., 1997; Zapun *et al*., 1998; Solda *et al*., 2006) have concluded that ERp57 has glycoprotein specificity mediated through its association with these lectin-chaperones. Our finding that Alb, the only nonglycosylated substrate examined in this study, was conspicuously excluded from those substrates affected by the loss of ERp57 is in good agreement with this view. Interestingly, the impact of ERp57 depletion varied among the glycoproteins examined. Whereas the effect was mild for αFP and α_2HS, the impact on TF was substantial. Molinari and coworkers recently examined the impact of ERp57 depletion on different glycoproteins and found that the severity of the defect in oxidative folding correlated with the dependency of the individual glycoprotein on the Cnx/Crt chaperone system for folding (Solda *et al*., 2006). Although the dependence on Cnx and Crt of the various secretory glycoproteins in the present study has not been rigorously examined, TF has been established as an obligate client of these chaperones (Wada *et al*., 1997), consistent with the strong impairment we observe upon ERp57 depletion. It is noteworthy that delays in oxidative folding were even detectable for αFP, α_2HS, and TF upon ERp57 depletion, given that all three glycoproteins were demonstrated to be substrates for PDI and that PDI was fully present when ERp57 was depleted. Recent studies from Jessop and coworkers have shed light on this issue (Jessop *et al*., 2009a). They speculated that entry of glycoproteins into the Cnx/Crt cycle might impede access of other PDI family members, even when ERp57 was depleted. Consistent with this view, they showed that the impaired oxidative folding of influenza HA observed upon ERp57 depletion could be largely bypassed if HA was prevented from associating with these chaperones.

There is some controversy as to whether ERp57 functions primarily as an isomerase or oxidase during protein folding. Previous studies by Jessop and coworkers, in which the disulfide content of HA was assessed through chemical alkylation, revealed that the HA produced in ERp57-deficient cells was fully oxidized but contained nonnative disulfides (Jessop *et al*., 2009a). This led to the conclusion that ERp57 functions primarily as an isomerase. Our current findings, as well as previous work showing that ERp57 deficiency slows the formation of fully oxidized class I heavy chains by as much as 10-fold (Zhang *et al*., 2006), point to a role for ERp57 in catalyzing disulfide formation but do not preclude the possibility of an additional role in isomerization. Future experiments using the chemical alkylation approach on secretory proteins in ERp57-depleted HepG2 cells will help to clarify this issue.

ERp72 is expected to possess a different substrate specificity compared with PDI or ERp57. The crystal structure of the ERp72 *bb′* domain fragment revealed that it lacks the hydrophobic face that is thought to mediate PDI interactions with nonnative substrates and, on the opposite face, lacks the positively charged patch that mediates ERp57 binding to Cnx and Crt (Kozlov *et al*., 2009). Consistent with a limited substrate specificity, a substrate trap mutant of ERp72 failed to stabilize a significant level of mixed disulfide complexes with substrates (Jessop *et al*., 2009b). Thus, our inability to detect any impact of ERp72 depletion is perhaps not surprising. Only when PDI was depleted in combination with ERp72 was a role for ERp72 revealed in the oxidative folding of Alb, a role previously masked by PDI in the single knockdown experiments. The lack of effect of this double knockdown on the three glycoprotein substrates further under-

scores the narrow substrate specificity of ERp72. It has been noted that when ERp57 is depleted (Solda *et al*., 2006) or the binding of Cnx or Crt to substrates is impeded through treatment with castanospermine (Jessop *et al*., 2009b) several glycoprotein substrates of ERp57 can shift to an association with ERp72, suggesting overlapping substrate specificities. However, we were unable to detect any involvement of ERp72 in the oxidative folding of αFP, α_2HS, or TF when ERp57 was depleted along with ERp72 or even in triple knockdowns lacking PDI, ERp57, and ERp72. It is possible that the engagement of these glycoproteins within the Cnx/Crt cycle precludes interactions with ERp72 or that ERp72 simply has a narrow substrate range not sampled in the present study.

Finally, we did not observe any impact on oxidative folding of depleting P5 alone or in combination with other PDI family members. These data suggest either a minor role for P5 or one specific for substrates not included in this study. P5 has previously been reported to be part of a multi-enzyme complex containing several ER chaperones including BiP (Meunier *et al*., 2002). In the substrate-trapping study by Jessop *et al*. (2009b), the authors confirmed a noncovalent interaction between P5 and BiP and reported mixed disulfide complexes between P5 and a broad range of substrates tested, although such complexes could only be observed when substrates were selectively translated in a semipermeabilized cell system. The authors speculated that in a manner analogous to ERp57 and Cnx/Crt, P5 is targeted to substrates via its interaction with BiP. Given that BiP interacts with many newly synthesized proteins in the ER including those in hepatoma cells (Molinari and Helenius, 2000; Schmidt and Perlmutter, 2005), the discrepancy between our respective findings may reflect differences in the methods used or may indicate that P5, although reported to have oxidase activity in vitro (Lappi *et al*., 2004), may act predominantly as a reductase to remove disulfide bonds in misfolded proteins targeted to BiP and degraded by ERAD (Jessop *et al*., 2009b).

The existence of a multi-enzyme complex containing PDI, ERp72, P5, BiP, and Grp94, but lacking Cnx, Crt, and ERp57, has led to the suggestion that the folding of various proteins may be segregated either spatially or temporally between different chaperone networks (Meunier *et al*., 2002) and that this may partially explain differences in PDI family member substrate specificity (Hatahet *et al*., 2009; Jessop *et al*., 2009b). Our data highlighting the apparent functional overlap of PDI and ERp72 in Alb oxidation as well as the lack of substrate sharing for ERp57 and ERp72 are in good agreement with such physical separation of function. However, our observation that both PDI and ERp57 are involved in the oxidative folding of most substrates tested is consistent with a more homogenous distribution of PDI family members in the ER. We also do not observe any impact of combined depletion of PDI and P5, which might have been expected if substrate selection was based on physical proximity of the oxidoreductases within a chaperone complex.

In summary, using a functional approach we have begun to define the relative roles of different PDI family members in oxidative protein folding within the ER. Although revealing in terms of delineating the predominant roles of PDI and ERp57 and the lesser impact of ERp72 and P5, it is noteworthy that disulfide formation still occurred even in the context of triple depletion conditions. An extension of this approach to other members of the PDI family should prove informative in revealing the sources of additional oxidase activities.

ACKNOWLEDGMENTS

We thank Dr. Tania Watts for the kind gift of antibodies. U.B. was supported by the CIHR Strategic Training Program in Membrane Proteins and L.A.R. was the recipient of an Ontario Graduate Scholarship. The authors gratefully acknowledge funding for this work by the Canadian Cancer Society and the Canadian Institutes of Health Research.

REFERENCES

Adeli, K., Wettesten, M., Asp, L., Mohammadi, A., Macri, J., and Olofsson, S.-O. (1997). Intracellular assembly and degradation of apolipoprotein B-100-containing lipoproteins in digitonin-permeabilized HEP G2 cells. J. Biol. Chem. *272*, 5031–5039.

Alanen, H. I., Salo, K. E., Pirneskoski, A., and Ruddock, L. W. (2006). pH dependence of the peptide thiol-disulfide oxidase activity of six members of the human protein disulfide isomerase family. Antioxid. Redox. Signal *8*, 283–291.

Appenzeller-Herzog, C., and Ellgaard, L. (2008). The human PDI family: versatility packed into a single fold. Biochim. Biophys. Acta *1783*, 535–548.

Appenzeller-Herzog, C., Riemer, J., Christensen, B., Sorensen, E. S., and Ellgaard, L. (2008). A novel disulphide switch mechanism in Ero1alpha balances ER oxidation in human cells. EMBO J. *27*, 2977–2987.

Bass, R., Ruddock, L. W., Klappa, P., and Freedman, R. B. (2004). A major fraction of endoplasmic reticulum-located glutathione is present as mixed disulfides with protein. J. Biol. Chem. *279*, 5257–5262.

Bulleid, N. J., and Freedman, R. B. (1988). Defective co-translational formation of disulphide bonds in protein disulphide-isomerase-deficient microsomes. Nature *335*, 649–651.

Chakravarthi, S., and Bulleid, N. J. (2004). Glutathione is required to regulate the formation of native disulfide bonds within proteins entering the secretory pathway. J. Biol. Chem. *279*, 39872–39879.

Danilczyk, U. G., and Williams, D. B. (2001). The lectin chaperone calnexin utilizes polypeptide-based interactions to associate with many of its substrates in vivo. J. Biol. Chem. *276*, 25532–25540.

Denisov, A. Y., Maattanen, P., Dabrowski, C., Kozlov, G., Thomas, D. Y., and Gehring, K. (2009). Solution structure of the bb′ domains of human protein disulfide isomerase. FEBS J. *276*, 1440–1449.

Forster, M. L., Sivick, K., Park, Y. N., Arvan, P., Lencer, W. I., and Tsai, B. (2006). Protein disulfide isomerase-like proteins play opposing roles during retrotranslocation. J. Cell Biol. *173*, 853–859.

Goldberger, R. F., Epstein, C. J., and Anfinsen, C. B. (1964). Purification and properties of a microsomal enzyme system catalyzing the reactivation of reduced ribonuclease and lysozyme. J. Biol. Chem. *239*, 1406–1410.

Hatahet, F., Ruddock, L. W., Ahn, K., Benham, A., Craik, D., Ellgaard, L., Ferrari, D., and Ventura, S. (2009). Protein disulfide isomerase: a critical evaluation of its function in disulfide bond formation. Antioxid. Redox. Signal *11*, 2807–2850.

Horibe, T., Iguchi, D., Masuoka, T., Gomi, M., Kimura, T., and Kikuchi, M. (2004). Replacement of domain b of human protein disulfide isomerase-related protein with domain b′ of human protein disulfide isomerase dramatically increases its chaperone activity. FEBS Lett. *566*, 311–315.

Ireland, B. S., Brockmeier, U., Howe, C. M., Elliott, T., and Williams, D. B. (2008). Lectin-deficient calreticulin retains full functionality as a chaperone for class I histocompatibility molecules. Mol. Biol. Cell *19*, 2413–2423.

Jansens, A., van Duijn, E., and Braakman, I. (2002). Coordinated nonvectorial folding in a newly synthesized multidomain protein. Science *298*, 2401–2403.

Jessop, C. E., Chakravarthi, S., Garbi, N., Hammerling, G. J., Lovell, S., and Bulleid, N. J. (2007). ERp57 is essential for efficient folding of glycoproteins sharing common structural domains. EMBO J. *26*, 28–40.

Jessop, C. E., Tavender, T. J., Watkins, R. H., Chambers, J. E., and Bulleid, N. J. (2009a). Substrate specificity of the oxidoreductase ERp57 is determined primarily by its interaction with calnexin and calreticulin. J. Biol. Chem. *284*, 2194–2202.

Jessop, C. E., Watkins, R. H., Simmons, J. J., Tasab, M., and Bulleid, N. J. (2009b). Protein disulphide isomerase family members show distinct substrate specificity: P5 is targeted to BiP client proteins. J. Cell Sci. *122*, 4287–4295.

Kang, K., Park, B., Oh, C., Cho, K., and Ahn, K. (2009). A role for protein disulfide isomerase in the early folding and assembly of MHC class I molecules. Antioxid. Redox. Signal *11*, 2553–2561.

Kemmink, J., Darby, N. J., Dijkstra, K., Nilges, M., and Creighton, T. E. (1997). The folding catalyst protein disulfide isomerase is constructed of active and inactive thioredoxin modules. Curr. Biol. *7*, 239–245.

Klappa, P., Ruddock, L. W., Darby, N. J., and Freedman, R. B. (1998). The b′ domain provides the principal peptide-binding site of protein disulfide isomerase but all domains contribute to binding of misfolded proteins. EMBO J. *17*, 927–935.

Kozlov, G., Maattanen, P., Schrag, J. D., Hura, G. L., Gabrielli, L., Cygler, M., Thomas, D. Y., and Gehring, K. (2009). Structure of the noncatalytic domains and global fold of the protein disulfide isomerase ERp72. Structure *17*, 651–659.

Kozlov, G., Maattanen, P., Schrag, J. D., Pollock, S., Cygler, M., Nagar, B., Thomas, D. Y., and Gehring, K. (2006). Crystal structure of the bb′ domains of the protein disulfide isomerase ERp57. Structure *14*, 1331–1339.

Kulp, M. S., Frickel, E. M., Ellgaard, L., and Weissman, J. S. (2006). Domain architecture of protein-disulfide isomerase facilitates its dual role as an oxidase and an isomerase in Ero1p-mediated disulfide formation. J. Biol. Chem. *281*, 876–884.

Laboissiere, M. C., Sturley, S. L., and Raines, R. T. (1995). The essential function of protein-disulfide isomerase is to unscramble non-native disulfide bonds. J. Biol. Chem. *270*, 28006–28009.

Land, A., Zonneveld, D., and Braakman, I. (2003). Folding of HIV-1 envelope glycoprotein involves extensive isomerization of disulfide bonds and conformation-dependent leader peptide cleavage. FASEB J. *17*, 1058–1067.

Lappi, A. K., Lensink, M. F., Alanen, H. I., Salo, K. E., Lobell, M., Juffer, A. H., and Ruddock, L. W. (2004). A conserved arginine plays a role in the catalytic cycle of the protein disulphide isomerases. J. Mol. Biol. *335*, 283–295.

Lee, S. O., Cho, K., Cho, S., Kim, I., Oh, C., and Ahn, K. (2010). Protein disulphide isomerase is required for signal peptide peptidase-mediated protein degradation. EMBO J. *29*, 363–375.

Linnik, K. M., and Herscovitz, H. (1998). Multiple molecular chaperones interact with apolipoprotein B during its maturation. The network of endoplasmic reticulum-resident chaperones (ERp72, GRP94, calreticulin, and BiP) interacts with apolipoprotein b regardless of its lipidation state. J. Biol. Chem. *273*, 21368–21373.

Lyles, M. M., and Gilbert, H. F. (1991). Catalysis of the oxidative folding of ribonuclease A by protein disulfide isomerase: pre-steady-state kinetics and the utilization of the oxidizing equivalents of the isomerase. Biochemistry *30*, 619–625.

Maruri-Avidal, L., Lopez, S., and Arias, C. F. (2008). Endoplasmic reticulum chaperones are involved in the morphogenesis of rotavirus infectious particles. J. Virol. *82*, 5368–5380.

Mazzarella, R. A., Srinivasan, M., Haugejorden, S. M., and Green, M. (1990). ERp72, an abundant luminal endoplasmic reticulum protein, contains three copies of the active site sequences of protein disulfide isomerase. J. Biol. Chem. *265*, 1094–1101.

Menon, S., Lee, J., Abplanalp, W. A., Yoo, S. E., Agui, T., Furudate, S., Kim, P. S., and Arvan, P. (2007). Oxidoreductase interactions include a role for ERp72 engagement with mutant thyroglobulin from the rdw/rdw rat dwarf. J. Biol. Chem. *282*, 6183–6191.

Meunier, L., Usherwood, Y. K., Chung, K. T., and Hendershot, L. M. (2002). A subset of chaperones and folding enzymes form multiprotein complexes in endoplasmic reticulum to bind nascent proteins. Mol. Biol. Cell *13*, 4456–4469.

Mezghrani, A., Fassio, A., Benham, A., Simmen, T., Braakman, I., and Sitia, R. (2001). Manipulation of oxidative protein folding and PDI redox state in mammalian cells. EMBO J. *20*, 6288–6296.

Molinari, M., and Helenius, A. (2000). Chaperone selection during glycoprotein translocation into the endoplasmic reticulum. Science *288*, 331–333.

Norgaard, P., Westphal, V., Tachibana, C., Alsoe, L., Holst, B., and Winther, J. R. (2001). Functional differences in yeast protein disulfide isomerases. J. Cell Biol. *152*, 553–562.

Oliver, J. D., Roderick, H. L., Llewellyn, D. H., and High, S. (1999). ERp57 functions as a subunit of specific complexes formed with the ER lectins calreticulin and calnexin. Mol. Biol. Cell *10*, 2573–2582.

Oliver, J. D., van der Wal, F. J., Bulleid, N. J., and High, S. (1997). Interaction of the thiol-dependent reductase ERp57 with nascent glycoproteins. Science *275*, 86–88.

Otsu, M., Bertoli, G., Fagioli, C., Guerini-Rocco, E., Nerini-Molteni, S., Ruffato, E., and Sitia, R. (2006). Dynamic retention of Ero1alpha and Ero1beta in the endoplasmic reticulum by interactions with PDI and ERp44. Antioxid. Redox. Signal *8*, 274–282.

Park, B., Lee, S., Kim, E., Cho, K., Riddell, S. R., Cho, S., and Ahn, K. (2006). Redox regulation facilitates optimal peptide selection by MHC class I during antigen processing. Cell *127*, 369–382.

Peaper, D. R., Wearsch, P. A., and Cresswell, P. (2005). Tapasin and ERp57 form a stable disulfide-linked dimer within the MHC class I peptide-loading complex. EMBO J. *24*, 3613–3623.

Pirneskoski, A., Klappa, P., Lobell, M., Williamson, R. A., Byrne, L., Alanen, H. I., Salo, K. E., Kivirikko, K. I., Freedman, R. B., and Ruddock, L. W. (2004). Molecular characterization of the principal substrate binding site of the ubiquitous folding catalyst protein disulfide isomerase. J. Biol. Chem. *279*, 10374–10381.

Rupp, K., Birnbach, U., Lundstrom, J., Van, P. N., and Soling, H. D. (1994). Effects of CaBP2, the rat analog of ERp72, and of CaBP1 on the refolding of denatured reduced proteins. Comparison with protein disulfide isomerase. J. Biol. Chem. *269*, 2501–2507.

Schelhaas, M., Malmstrom, J., Pelkmans, L., Haugstetter, J., Ellgaard, L., Grunewald, K., and Helenius, A. (2007). Simian Virus 40 depends on ER protein folding and quality control factors for entry into host cells. Cell *131*, 516–529.

Schmidt, B. Z., and Perlmutter, D. H. (2005). Grp78, Grp94, and Grp170 interact with alpha1-antitrypsin mutants that are retained in the endoplasmic reticulum. Am. J. Physiol. Gastrointest. Liver Physiol. *289*, G444–G455.

Sevier, C. S., and Kaiser, C. A. (2002). Formation and transfer of disulphide bonds in living cells. Nat. Rev. Mol. Cell Biol. *3*, 836–847.

Sevier, C. S., and Kaiser, C. A. (2008). Ero1 and redox homeostasis in the endoplasmic reticulum. Biochim. Biophys. Acta *1783*, 549–556.

Solda, T., Garbi, N., Hammerling, G. J., and Molinari, M. (2006). Consequences of ERp57 deletion on oxidative folding of obligate and facultative clients of the calnexin cycle. J. Biol. Chem. *281*, 6219–6226.

Tian, G., Xiang, S., Noiva, R., Lennarz, W. J., and Schindelin, H. (2006). The crystal structure of yeast protein disulfide isomerase suggests cooperativity between its active sites. Cell *124*, 61–73.

Wada, I., Kai, M., Imai, S., Sakane, F., and Kanoh, H. (1997). Promotion of transferrin folding by cyclic interactions with calnexin and calreticulin. EMBO J. *16*, 5420–5432.

Walker, K. W., and Gilbert, H. F. (1997). Scanning and escape during protein-disulfide isomerase-assisted protein folding. J. Biol. Chem. *272*, 8845–8848.

Wang, L., Li, S. J., Sidhu, A., Zhu, L., Liang, Y., Freedman, R. B., and Wang, C. C. (2009). Reconstitution of human Ero1-L{alpha}/protein-disulfide isomerase oxidative folding pathway in vitro: Position-dependent differences in role between the a and a′ domains of protein disulfide isomerase. J. Biol. Chem. *284*, 199–206.

Weissman, J. S., and Kim, P. S. (1993). Efficient catalysis of disulphide bond rearrangements by protein disulphide isomerase. Nature *365*, 185–188.

Williams, D. B. (2006). Beyond lectins: the calnexin/calreticulin chaperone system of the endoplasmic reticulum. J. Cell Sci. *119*, 615–623.

Wu, J., and Kaufman, R. J. (2006). From acute ER stress to physiological roles of the Unfolded Protein Response. Cell Death Differ. *13*, 374–384.

Xiao, R., Wilkinson, B., Solovyov, A., Winther, J. R., Holmgren, A., Lundstrom-Ljung, J., and Gilbert, H. F. (2004). The contributions of protein disulfide isomerase and its homologues to oxidative protein folding in the yeast endoplasmic reticulum. J. Biol. Chem. *279*, 49780–49786.

Yoshida, H. (2007). Unconventional splicing of XBP-1 mRNA in the unfolded protein response. Antioxid. Redox. Signal *9*, 2323–2333.

Zapun, A., Darby, N. J., Tessier, D. C., Michalak, M., Bergeron, J. J., and Thomas, D. Y. (1998). Enhanced catalysis of ribonuclease B folding by the interaction of calnexin or calreticulin with ERp57. J. Biol. Chem. *273*, 6009–6012.

Zhang, Y., Baig, E., and Williams, D. B. (2006). Functions of ERp57 in the folding and assembly of major histocompatibility complex class I molecules. J. Biol. Chem. *281*, 14622–14631.

Zhang, Y., Kozlov, G., Pocanschi, C. L., Brockmeier, U., Ireland, B. S., Maattanen, P., Howe, C., Elliott, T., Gehring, K., and Williams, D. B. (2009). ERp57 does not require interactions with calnexin and calreticulin to promote assembly of class I histocompatibility molecules, and it enhances peptide loading independently of its redox activity. J. Biol. Chem. *284*, 10160–10173.

Zheng, L., Baumann, U., and Reymond, J. L. (2004). An efficient one-step site-directed and site-saturation mutagenesis protocol. Nucleic Acids Res. *32*, e115.